JACS
JOURNAL OF THE AMERICAN CHEMICAL SOCIETY
pubs.acs.org/JACS
Communication

Thermal Cycling of a MOF-Based NO Disproportionation Catalyst

Ashley M. Wright, Chenyue Sun, and Mircea Dincă*

Cite This: https://dx.doi.org/10.1021/jacs.0c12134
Read Online
ACCESS | Metrics & More | Article Recommendations | Supporting Information

ABSTRACT: The metal−organic framework Cu^{I}-MFU-4*l* reacts with NO, initially forming a copper(I)-nitrosyl at low pressure, and subsequently generates NO disproportionation products Cu^{II}−NO_2 and N_2O. The thermal stability of MFU-4*l* allows NO_x to be released from the framework at temperatures greater than 200 °C. This treatment regenerates the original Cu^{I}-MFU-4*l*, which can engage in subsequent cycles of NO disproportionation.

Noxa, the Latin for "hurt" or "injury," is the etymological root of *noxious*, a word that might as well be derived from NO_x, the communal name for the noxious oxides of nitrogen. A class of pollutants emitted by combustion engines, NO_x have a lasting negative impact on the environment and human health.[1,2] Despite significant advances in mitigating automobile emissions through technologies such as the three-way catalytic converter, transportation still contributes nearly half of all NO_x emissions.[3] Consequently, new NO_x abatement systems are needed, particularly as stricter automobile emission regulations come into effect.[3,4] Even though current new technologies like selective catalytic reduction (SCR) and NO_x adsorber catalysts are effective in reducing tailpipe NO_x emissions, SCR catalysts must operate at temperatures exceeding 200 °C to achieve the optimal reduction of 97% NO_x.[5] However, catalyst beds, especially in diesel and lean-burn engines, do not reach this optimal temperature for several minutes after an engine cold-start, which leads to an initial NO_x emissions spike.[6] This initial spike is sufficiently significant to potentially cause failed emission tests under more stringent emission standards and must be addressed independently of the NO_x emissions during steady-state engine operation. A potential solution to this challenge is the development of a method that stores NO_x at low temperature (i.e., <200 °C), while the main catalyst bed reaches its optimal operating temperature, and then releases NO_x back into the catalyst system at temperatures higher than 200 °C.[7−9]

One method to capture NO_x, at least partially, is to enable NO disproportionation at a metal site by allowing three NO molecules to react and generate N_2O and a bound metal-nitrite:

$$3NO + M^{n} \rightarrow M^{n+1}{-}NO_2 + N_2O$$

This process corresponds to a two-third reduction of the overall NO_x emissions at low temperatures. Although thermodynamically favorable (ΔG° = −24.6 kcal/mol), NO disproportionation is kinetically sluggish and generally requires a catalyst or high pressures to proceed.[10,11] Potential catalysts include transition metal complexes such as species containing Mn,[12,13] Fe,[14−16] Co,[17,18] Ni,[19] and Cu.[20−27]

Metal−organic frameworks (MOFs) are porous crystalline materials and can contain metal sites that display reactivity toward small molecules like NO. Here, we show that $Zn_3Cu^{I}_2Cl_2(BTDD)_3$ (Cu^{I}-MFU-4*l*; H_2BTDD = bis(1H-1,2,3-triazolo[4,5-b;4′,5′-i])dibenzo[1,4]dioxin),[28−32] a MOF featuring Cu^{I} sites in site-isolated coordination environments (Figure 1) reminiscent of the NO-disproportionation complexes $TpCu^{I}$ (Tp = tris(pyrazol-1-yl)hydroborate),[20,21] performs NO disproportionation at low NO concentration. Critically, the thermal stability of MFU-4*l* allows for the starting Cu^{I} material to be regenerated through thermal release of NO_x from the resulting Cu^{II}-nitrite at high temperature. These results demonstrate a potentially attractive scheme for cold-start NO capture.

Armed with the knowledge of previous reports of NO binding in the MFU-4*l* family[33,34] and of NO disproportionation at molecular Tp metal complexes, we initiated our study by investigating how the material properties such as cation identity and oxidation state influence the NO sorption profile in M-MFU-4*l* (M = Cu, Zn) (Figure 2). The parent Zn-MFU-4*l*, featuring tetrahedral $N_3Zn{-}Cl$ sites, adsorbs the lowest amount, 0.51 mmol NO/g at 750 Torr. The low NO uptake is likely due to a weak physisorption interaction with the framework, the saturated coordination environment around Zn preventing a stronger metal−NO interaction.

$Zn_3Cu^{II}_2Cl_4(BTDD)_3$ (Cu^{II}-MFU-4*l*), accessible by exchanging two Zn^{II} atoms in original MFU-4*l* with Cu^{II} (Figure 1),[31] adsorbs 1.43 mmol NO/g at 750 Torr, significantly more NO than MFU-4*l*. This is not surprising: Cu^{II} is much less accommodating of a tetrahedral coordination environment, and the $N_3Cu{-}Cl$ geometry is likely sufficiently distorted[35,36] to allow NO to approach much closer and enable a stronger interaction with Cu^{II} than with Zn^{II}, although still weak enough to enable reversible NO desorption without hysteresis (Figure

Received: November 19, 2020

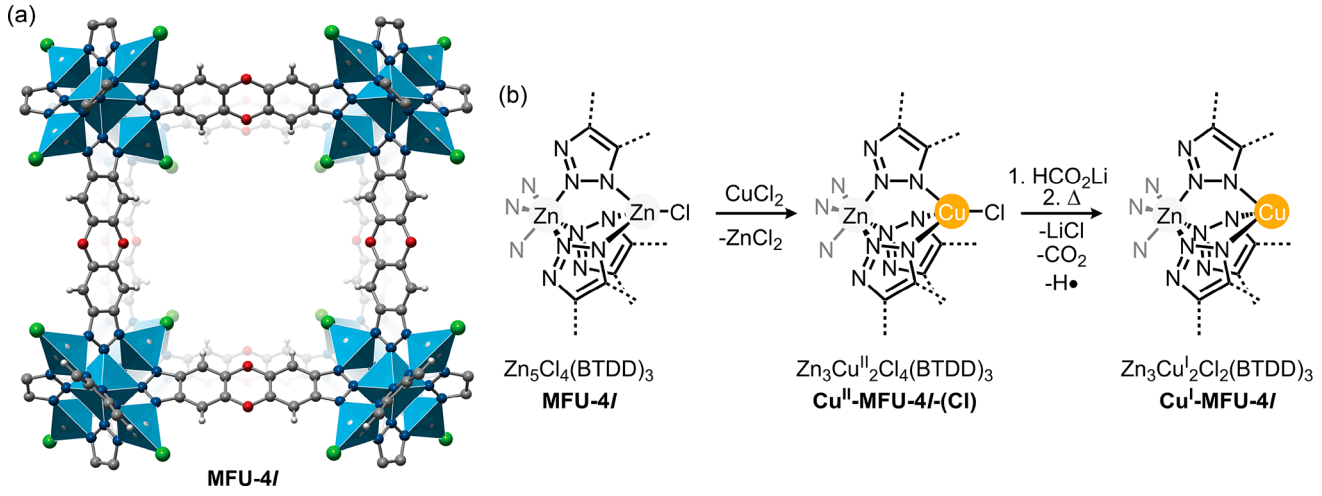

Figure 1. (a) Crystal structure of MFU-4*l* showing the small pore with eight zinc chloride vertices (Zn, blue polyhedra; Cl, green; O, red; N, dark blue; C, dark gray; H, white). (b) Synthetic scheme for the installation of a Cu^{I} center at the secondary building unit of MFU-4*l*.[31]

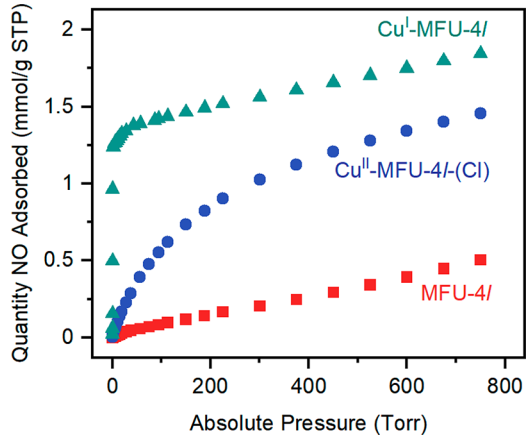

Figure 2. NO adsorption isotherms for MFU-4*l* (red squares), Cu^{II}-MFU-4*l*-(Cl) (blue circles), and Cu^{I}-MFU-4*l* (green triangles) measured at 298 K. Additional isotherm data are found in Figures S7–S9.

2). Variable temperature NO isotherms fitted to the dual-site Langmuir model revealed a coverage-dependent isosteric enthalpy of adsorption (ΔH_{ads}) curve that starts at −37 kJ/mol at zero-coverage and remains flat up to ∼0.5 mmol/g, whereupon it gradually decreases to −19 kJ/mol over the 0.5–1.5 mmol/g range (Figures S11 and S12). The relatively low zero-coverage enthalpy of adsorption indicates a weak Cu^{II}–NO interaction, as also observed in molecular Cu^{II} nitrosyl species.[37,38]

The formation of a weak Cu^{II}-nitrosyl species was confirmed by vibrational spectroscopy. Diffuse reflectance infrared Fourier transform spectroscopy (DRIFTS) of Cu^{II}-MFU-4*l* exposed to increasing concentrations of NO in Ar (ranging from 0.5–5% v/v) indicates the growth of a band at 1846 cm^{-1}, only slightly red-shifted relative to free NO at 1875 cm^{-1} (Figure S14). For comparison, HKUST-1, a MOF featuring dicopper(II) paddlewheel units capable of weakly binding NO, features a Cu^{II}–NO species with ν_{NO} = 1887 cm^{-1}.[39] Likewise, structurally characterized molecular complexes, $[Cu^{II}(NO)(MeNO_2)_5][PF_6]_2$ and $[TBA][Cu^{II}(NO)Cl_3]$, exhibit NO stretches at 1930 and 1834 cm^{-1}, respectively.[37,38,40] Notably, the band at 1846 cm^{-1} does not change upon continued

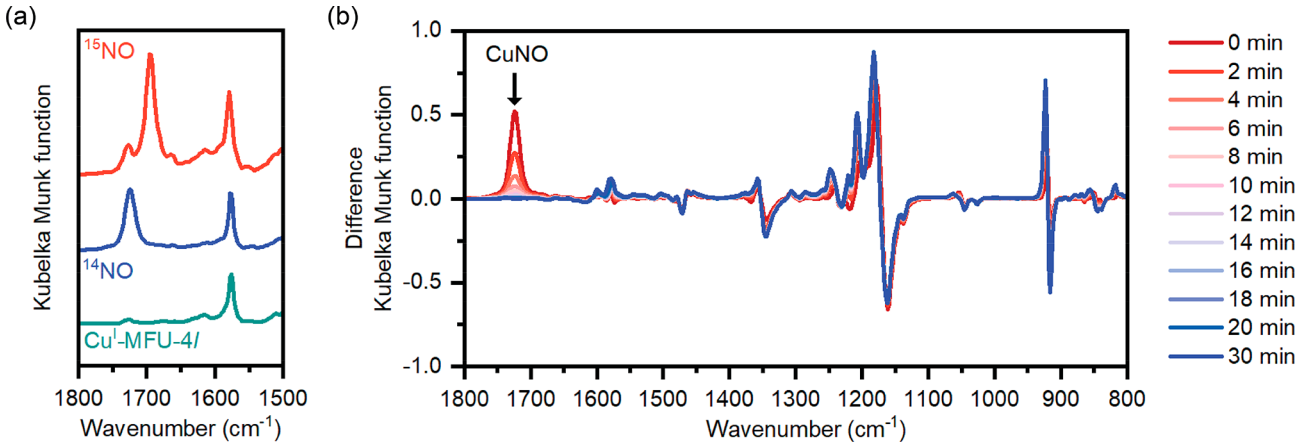

Figure 3. (a) DRIFTS of Cu^{I}-MFU-4*l* (green trace), Cu^{I}-MFU-4*l* exposed to ^{14}NO (blue trace) and Cu^{I}-MFU-4*l* exposed to ^{15}NO (red trace). (b) DRIFTS difference spectra showing the time course of the reaction between Cu^{I}-MFU-4*l* and a stream of 1% NO in argon (flow rate 100 sccm). The zero-time spectrum is recorded immediately after NO addition, presumably when the Cu(NO) concentration is maximum. This band gradually decreases with time due to the NO disproportionation reaction.

https://dx.doi.org/10.1021/jacs.0c12134
J. Am. Chem. Soc. XXXX, XXX, XXX–XXX

exposure of Cu^{II}-MFU-4*l* to NO, but disappears upon purging the sample with Ar (Figure S15), confirming that NO binding to Cu^{II}-MFU-4*l* is indeed weak and reversible, consistent with the adsorption and desorption data.

Formal reduction of Cu^{II} to Cu^{I} with concomitant loss of chloride[31] causes a significant improvement in the low-pressure NO uptake, with Cu^{I}-MFU-4*l* adsorbing 1.24 mmol/g below 1.4 Torr. This uptake is 3 orders of magnitude greater than that of Cu^{II}-MFU-4*l* (0.008 mmol/g) and original MFU-4*l* (0.002 mmol/g) at the same pressure (Figure 2). The NO isotherm for Cu^{I}-MFU-4*l* rapidly plateaus above ~1.5 Torr (1.2 mmol/g, Figure S10), reaches 1.84 mmol NO/g at 760 Torr at 298 K, and is notably hysteretic upon desorption. A 1:1 ratio of NO:Cu^{I} (1.70 mmol NO/g) is reached at 525 Torr. We assign the steep, hysteretic uptake of NO here to a strong binding interaction between Cu^{I} and NO, in line with previous observations of strong binding of small molecules such as ethylene, propylene, and carbon monoxide at the open Cu^{I} sites in Cu^{I}-MFU-4*l*.[31,33,41]

To gain deeper insight into the nature of the NO binding to Cu^{I}-MFU-4*l*, we once again used DRIFTS. Flowing a relatively dilute stream of NO (10−10 000 ppm in Ar) over a powder sample of Cu^{I}-MFU-4*l* results in the appearance of a new band at 1726 cm^{-1}, which shifts to 1692 cm^{-1} when ^{15}NO is used (Δ = 34 cm^{-1}; expected shift from Hooke's law = 33 cm^{-1}) (Figure 3a). We assign this band to a copper(I) nitrosyl species based on comparable IR bands in molecular copper(I)-nitrosyl complexes with similar coordination environments, such as $Tp^{tBu}Cu(NO)$ (1712 cm^{-1}) and $Tp^{Ph}Cu(NO)$ (1720 cm^{-1}).[21,42] In the context of cold-start NO_x emissions, it is particularly noteworthy that NO binds to Cu^{I}-MFU-4*l* at concentrations as low as 10 ppm in Ar (Figure S19).

Remarkably, exposure to more concentrated NO streams (1% in Ar) causes loss of the band at 1726 cm^{-1} and formation of several new spectral features over a span of approximately 30 min (Figure 3b). Because many of these new spectral features overlap with bands pertaining to the MOF itself, we identified those relevant to the NO transformations by monitoring the reaction using both natural-abundance NO, and isotopically labeled ^{15}NO (Figure S17). Comparison of the difference spectra at the end of the reaction revealed two bands that are isotopically sensitive, 1284 cm^{-1} (1261 cm^{-1}, Δ = 23 cm^{-1}) and 879 cm^{-1} (873 cm^{-1}, Δ = 6 cm^{-1}) (Figure S18). We assign these bands to the asymmetric and bending vibrations of a copper(II)-nitrite, respectively. Molecular $Tp^{Ms,H}Cu(O_2N)$ features nitrite bands at similar positions: 1288 (ν_a), 1184 (ν_s), and 880 (δ_a) cm^{-1}.[21] The expected region (1200−1150 cm^{-1}) of the NO_2^- symmetric stretch, ν_s, is obscured by a more intense vibrational band from the MOF. The spectral features of this reaction product are consistent with an *O*,*O*′-nitrito isomer,[21,43] formed from NO disproportionation, $3NO \rightarrow NO_2 + N_2O$, with the Cu^{I} center both mediating the reaction and retaining the product NO_2 in the solid state to form Cu^{II}-MFU-4*l*-(NO_2) (Scheme 1).[21] Under the reaction conditions explored, we were not able to identify any vibrational bands associated with an intermediate species, such as a hyponitrite.[15,26,27,44] Further supporting NO disproportionation, analysis of the headspace using real time gas analysis mass spectrometry revealed generation of N_2O (Figure S28). Additionally, analysis of the reaction product, Cu^{II}-MFU-4*l*-(NO_2), by electron paramagnetic resonance (EPR) revealed a signal consistent with a Cu^{II} species (Figure S20). Overall, these results support a Cu^{I}-MFU-4*l* mediated NO disproportionation reaction.

Scheme 1. Proposed NO Disproportionation Cycle Using Cu^{I}-MFU-4*l*[a]

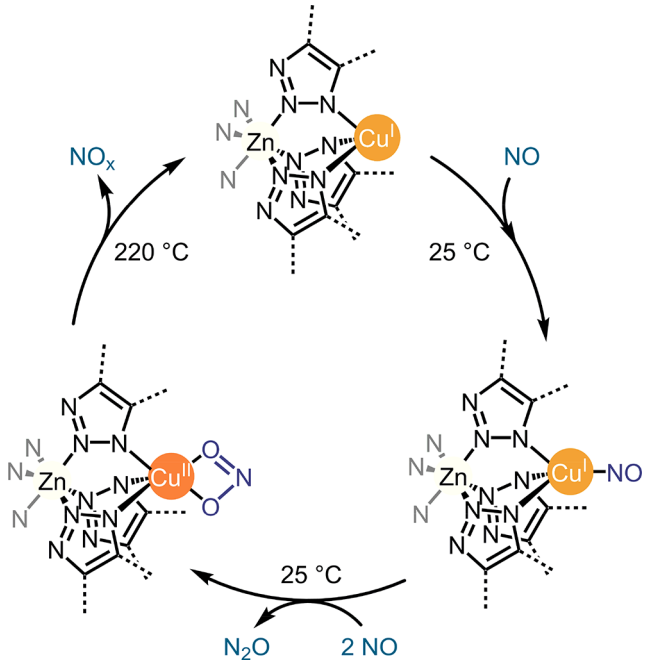

[a]During the thermal decomposition of Cu-MFU-4l(NO_2), NO is the major NO_x species detected.

Cu^{II}-MFU-4*l*-(NO_2) presents modest further uptake of NO (Figure 4a, red diamonds) of only 0.002 mmol/g at 1.5 Torr and 0.40 mmol/g at 750 Torr, significantly lower than Cu^{II}-MFU-4*l*-(Cl) and Cu^{I}-MFU-4*l*, but comparable to MFU-4*l*. We attribute the lower NO uptake in Cu^{II}-MFU-4*l*-(NO_2) to the bidentate *O*,*O*′-nitrito binding mode, which blocks the coordination sites at Cu^{II}.

Given the thermal stability of the Cu-MFU-4*l* materials, we hypothesized the Cu^{II}−nitrite bond could be homolyzed at high temperature, releasing an equivalent of NO_2 and regenerating Cu^{I}-MFU-4*l* (Scheme 1). Heating Cu^{II}-MFU-4*l*-(NO_2) at 240 °C under dynamic vacuum for 16 h results in a color change from green to beige, a discoloration characteristic of transitioning from Cu^{II} to Cu^{I}, which would indeed imply thermal release of one NO_2 equivalent and closure of a catalytic NO disproportionation cycle. NO sorption analysis of the beige solid revealed isotherm characteristics that are comparable to those of pristine Cu^{I}-MFU-4*l*, albeit with somewhat reduced low and high pressure capacities of 0.83 mmol/g and 1.41 mmol/g at 1.5 and 750 Torr, respectively, (Figure 4a).

Further insight into the nature of thermal regeneration of Cu^{I}-MFU-4*l* came from thermogravimetric analysis of Cu^{II}-MFU-4*l*-(NO_2), which revealed two partial mass loss events of ~2.4 and ~8.9 wt % at 150 and 220 °C, respectively, prior to framework degradation at temperatures greater than 300 °C (Figure S21). Evolved gas analysis via mass spectrometry (TGA-MS) revealed that, surprisingly, the major NO_x species released from Cu^{II}-MFU-4*l*-(NO_2) is NO (m/z = 30) at 220 °C, further supported by release of ^{15}NO (m/z = 31) from Cu-MFU-4*l*-($^{15}NO_2$). Indeed, we do not observe a m/z = 46 associated with NO_2. Evidently, the mechanism of regenerating

https://dx.doi.org/10.1021/jacs.0c12134
J. Am. Chem. Soc. XXXX, XXX, XXX−XXX

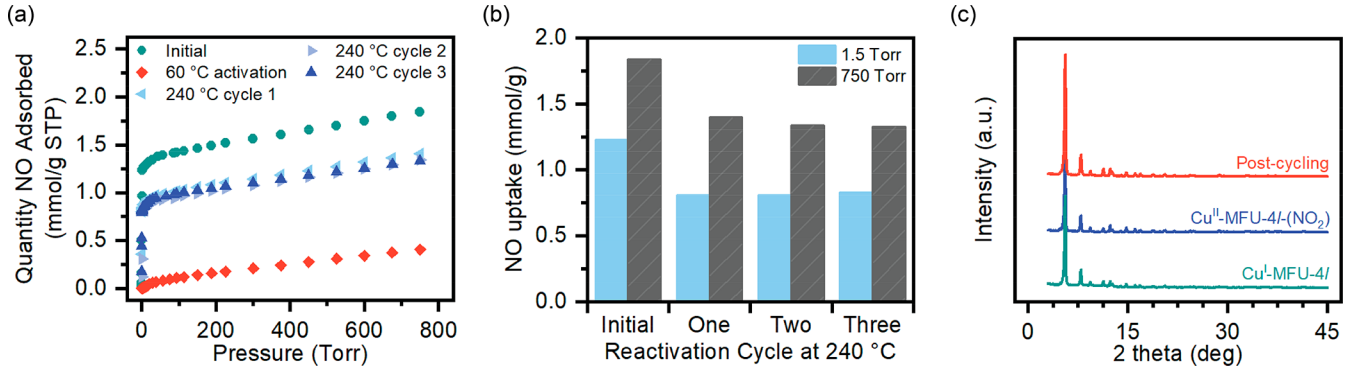

Figure 4. (a) NO isotherms of Cu-MFU-4*l* after NO/thermal treatment cycles. Green circles represent the NO isotherm of the activated Cu^{I}-MFU-4*l*, red circles denote Cu^{II}-MFU-4*l*-(NO_2), and various shaded blue triangles denote materials after NO exposure/240 °C thermal treatment cycles. (b) Bar graph showing the NO uptake at 1.5 and 750 Torr after NO exposure/240 °C reactivation cycles. (c) PXRD patterns of activated Cu^{I}-MFU-4*l*, Cu^{II}-MFU-4*l*-(NO_2), and the material recovered after thermal treatment of Cu^{II}-MFU-4*l*-(NO_2) at 250 °C under a flow of N_2.

Cu^{I}-MFU-4*l* from Cu^{II}-MFU-4*l*-(NO_2) is not simple homoloysis of the Cu−NO_2 bond and may require more extensive future studies. We hypothesize that thermal release of the NO_2 equivalent instead occurs through evolution of NO through thermal decomposition of nitrite. Under our reaction conditions, at least one of the pathways in which this reactive species is reduced back to Cu^{I} is through oxidative decomposition of the framework. In agreement with this hypothesis, TGA-MS reveals a peak with m/z of 44, which after ^{15}N isotopic labeling of the nitrite and 2-position of the azolate ligand was determined to be CO_2 and not N_2O (Figures S22−S25).

The intricacies of the NO_2 release mechanism notwithstanding, the disproportionation of NO over Cu^{I}-MFU-4*l* is catalytic, as demonstrated by our recycling of the MOF over three cycles, with each complete cycle involving exposure of Cu^{I}-MFU-4*l* to NO at 25 °C for 16 h followed by heating to 240 °C under dynamic vacuum for 16 h. NO adsorption isotherms after each cycle revealed that despite an initial drop in NO uptake after the first cycle, the total NO uptake at 750 Torr remains approximately constant, ∼1.4 mmol/g, over three cycles (Figure 4a and b). Crucially, the stability of the material under the experimental conditions was further confirmed by powder X-ray diffraction (PXRD) and surface area analysis of catalyst recovered after the three NO disproportionation cycles. Thus, PXRD revealed peaks consistent with Cu-MFU-4*l* (Figure 4c), and fitting a 77 K N_2 adsorption isotherm to the BET equation revealed a surface area of 3091 m^2/g (Figure S6), only marginally lower than the surface area of pristine Cu-MFU-4*l* (3171 m^2/g) confirming retention of porosity.

The above results demonstrate that well-defined Cu^{I} sites in Cu^{I}-MFU-4*l* react with low concentrations of NO (10 ppm) and catalyze NO disproportionation. The high thermal stability of the framework allows for release of NO_x from the framework and regeneration of the starting material. The capture and disproportionation of NO can be repeated at least three times with only the first cycle causing a reduction in total NO uptake and no further loss in subsequent cycles. Future efforts will focus preparing a catalytic system with added reductants to prevent oxidative degradation of the framework.

■ ASSOCIATED CONTENT

Supporting Information

The Supporting Information is available free of charge at https://pubs.acs.org/doi/10.1021/jacs.0c12134.

Experimental details including powder X-ray diffraction, gas isotherms, TGA, EPR, and DRIFTS (PDF)

■ AUTHOR INFORMATION

Corresponding Author

Mircea Dincă − *Department of Chemistry, Massachusetts Institute of Technology, Cambridge, Massachusetts 02139, United States;* orcid.org/0000-0002-1262-1264; Email: mdinca@mit.edu

Authors

Ashley M. Wright − *Department of Chemistry, Massachusetts Institute of Technology, Cambridge, Massachusetts 02139, United States;* orcid.org/0000-0002-9475-2638

Chenyue Sun − *Department of Chemistry, Massachusetts Institute of Technology, Cambridge, Massachusetts 02139, United States*

Complete contact information is available at: https://pubs.acs.org/10.1021/jacs.0c12134

Author Contributions

All authors have given approval to the final version of the manuscript.

Notes

The authors declare no competing financial interest.

■ ACKNOWLEDGMENTS

This work was funded by the Ford Motor Company. We thank Luming Yang for assistance in collecting EPR spectra.

■ REFERENCES

(1) Boningari, T.; Smirniotis, P. G. Impact of Nitrogen Oxides on the Environment and Human Health: Mn-Based Materials for the NOx Abatement. *Curr. Opin. Chem. Eng.* **2016**, *13* (x), 133−141.

(2) Monks, P. S.; Granier, C.; Fuzzi, S.; Stohl, A.; Williams, M. L.; Akimoto, H.; Amann, M.; Baklanov, A.; Baltensperger, U.; Bey, I.; et al. Atmospheric Composition Change - Global and Regional Air Quality. *Atmos. Environ.* **2009**, *43* (33), 5268−5350.

(3) Granger, P.; Parvulescu, V. I. Catalytic NO x Abatement Systems for Mobile Sources: From Three-Way to Lean Burn after-Treatment Technologies. *Chem. Rev.* **2011**, *111* (5), 3155−3207.

(4) Environmental Protection Agency. Control of Air Pollution from Motor Vehicles: Tier 3 Motor Vehicle Emission and Fuel Standards; Final Rule. *Fed. Regist.* **2014**, *79*, 23414−23886.

(5) Chen, H.-Y.; Mulla, S.; Weigert, E.; Camm, K.; Ballinger, T.; Cox, J.; Blakeman, P. Cold Start Concept (CSC™): A Novel Catalyst

for Cold Start Emission Control. *SAE Int. J. Fuels Lubr.* **2013**, *6* (2), 372−381.
(6) Johnson, T. Vehicular Emissions in Review. *SAE Int. J. Engines* **2013**, *6* (2), 699−715.
(7) Liu, G.; Gao, P. X. A Review of NOx Storage/Reduction Catalysts: Mechanism, Materials and Degradation Studies. *Catal. Sci. Technol.* **2011**, *1* (4), 552−568.
(8) Gu, Y.; Epling, W. S. Passive NOx Adsorber: An Overview of Catalyst Performance and Reaction Chemistry. *Appl. Catal., A* **2019**, *570*, 1−14.
(9) Ryou, Y.; Lee, J.; Lee, H.; Kim, C. H.; Kim, D. H. Effect of Various Activation Conditions on the Low Temperature NO Adsorption Performance of Pd/SSZ-13 Passive NOx Adsorber. *Catal. Today* **2019**, *320* (x), 175−180.
(10) Melia, T. P. Decomposition of Nitric Oxide at Elevated Pressures. *J. Inorg. Nucl. Chem.* **1965**, *27* (1), 95−98.
(11) Agnew, S. F.; Swanson, B. I.; Jones, L. H.; Mills, R. L. Disproportionation of Nitric Oxide at High Pressure. *J. Phys. Chem.* **1985**, *89* (9), 1678−1682.
(12) Franz, K. J.; Lippard, S. J. Disproportionation of Nitric Oxide Promoted by a Mn Tropocoronand. *J. Am. Chem. Soc.* **1998**, *120* (35), 9034−9040.
(13) Martirosyan, G. G.; Azizyan, A. S.; Kurtikyan, T. S.; Ford, P. C. Low Temperature NO Disproportionation by Mn Porphyrin. Spectroscopic Characterization of the Unstable Nitrosyl Nitrito Complex MnIII(TPP)(NO)(ONO). *Chem. Commun.* **2004**, *4* (13), 1488.
(14) Franz, K. J.; Lippard, S. J. NO Disproportionation Reactivity of Fe Tropocoronand Complexes. *J. Am. Chem. Soc.* **1999**, *121* (45), 10504−10512.
(15) Brozek, C. K.; Miller, J. T.; Stoian, S. A.; Dincă, M. NO Disproportionation at a Mononuclear Site-Isolated Fe2+ Center in Fe2+-MOF-5. *J. Am. Chem. Soc.* **2015**, *137* (23), 7495−7501.
(16) Jover, J.; Brozek, C. K.; Dincă, M.; López, N. Computational Exploration of NO Single-Site Disproportionation on Fe-MOF-5. *Chem. Mater.* **2019**, *31* (21), 8875−8885.
(17) Gwost, D.; Caulton, K. G. Oxidation of Coordinated Nitric Oxide by Free Nitric Oxide. *Inorg. Chem.* **1974**, *13* (2), 414−417.
(18) Miki, E. Reaction of Bis(8-Quinolinolate)Nitrosyl Cobalt with Nitrogen Oxide. *Chem. Lett.* **1980**, *9* (7), 835−838.
(19) Wright, A. M.; Zaman, H. T.; Wu, G.; Hayton, T. W. Mechanistic Insights into the Formation of N2O by a Nickel Nitrosyl Complex. *Inorg. Chem.* **2014**, *53* (6), 3108−3116.
(20) Ruggiero, C. E.; Carrier, S. M.; Tolman, W. B. Reductive Disproportionation of NO Mediated by Copper Complexes: Modeling N2O Generation by Copper Proteins and Heterogeneous Catalysts. *Angew. Chem., Int. Ed. Engl.* **1994**, *33* (8), 895−897.
(21) Schneider, J. L.; Carrier, S. M.; Ruggiero, C. E.; Young, V. G.; Tolman, W. B. Influences of Ligand Environment on the Spectroscopic Properties and Disproportionation Reactivity of Copper-Nitrosyl Complexes. *J. Am. Chem. Soc.* **1998**, *120* (44), 11408−11418.
(22) Shimokawabe, M.; Okumura, K.; Ono, H.; Takezawa, N. N2O and NO2 Formation in the Disproportionation of NO over Ion Exchanged Cu-ZSM-5 at Lower Temperature. *React. Kinet. Catal. Lett.* **2001**, *73* (2), 267−274.
(23) Lionetti, D.; de Ruiter, G.; Agapie, T. A Trans -Hyponitrite Intermediate in the Reductive Coupling and Deoxygenation of Nitric Oxide by a Tricopper-Lewis Acid Complex. *J. Am. Chem. Soc.* **2016**, *138* (15), 5008−5011.
(24) Metz, S. N2O Formation via Reductive Disproportionation of NO by Mononuclear Copper Complexes: A Mechanistic DFT Study. *Inorg. Chem.* **2017**, *56* (7), 3820−3833.
(25) Alternative reduction pathways of NO include reduction of NO to N_2O and H_2O in the presence of protons and an electron source. This is how NO reductase reduces NO, the hyponitrite intermediate is intercepted by a proton transfer. See refs 26 and 27.
(26) Wijeratne, G. B.; Hematian, S.; Siegler, M. A.; Karlin, K. D. Copper(I)/NO (g) Reductive Coupling Producing a Trans -Hyponitrite Bridged Dicopper(II) Complex: Redox Reversal Giving Copper(I)/NO (g) Disproportionation. *J. Am. Chem. Soc.* **2017**, *139* (38), 13276−13279.
(27) Wijeratne, G. B.; Bhadra, M.; Siegler, M. A.; Karlin, K. D. Copper(I) Complex Mediated Nitric Oxide Reductive Coupling: Ligand Hydrogen Bonding Derived Proton Transfer Promotes N 2 O (g) Release. *J. Am. Chem. Soc.* **2019**, *141* (45), 17962−17967.
(28) Denysenko, D.; Grzywa, M.; Tonigold, M.; Streppel, B.; Krkljus, I.; Hirscher, M.; Mugnaioli, E.; Kolb, U.; Hanss, J.; Volkmer, D. Elucidating Gating Effects for Hydrogen Sorption in MFU-4-Type Triazolate-Based Metal-Organic Frameworks Featuring Different Pore Sizes. *Chem. - Eur. J.* **2011**, *17* (6), 1837−1848.
(29) Denysenko, D.; Werner, T.; Grzywa, M.; Puls, A.; Hagen, V.; Eickerling, G.; Jelic, J.; Reuter, K.; Volkmer, D. Reversible Gas-Phase Redox Processes Catalyzed by Co-Exchanged MFU-4l(Arge). *Chem. Commun.* **2012**, *48* (9), 1236−1238.
(30) Denysenko, D.; Jelic, J.; Reuter, K.; Volkmer, D. Postsynthetic Metal and Ligand Exchange in MFU-4 L: A Screening Approach toward Functional Metal-Organic Frameworks Comprising Single-Site Active Centers. *Chem. - Eur. J.* **2015**, *21* (22), 8188−8199.
(31) Denysenko, D.; Grzywa, M.; Jelic, J.; Reuter, K.; Volkmer, D. Scorpionate-Type Coordination in MFU-4 l Metal-Organic Frameworks: Small-Molecule Binding and Activation upon the Thermally Activated Formation of Open Metal Sites. *Angew. Chem., Int. Ed.* **2014**, *53* (23), 5832−5836.
(32) Brozek, C. K.; Dincă, M. Cation Exchange at the Secondary Building Units of Metal-Organic Frameworks. *Chem. Soc. Rev.* **2014**, *43* (16), 5456−5467.
(33) Li, L.; Yang, Y.; Mohamed, M. H.; Zhang, S.; Veser, G.; Rosi, N. L.; Johnson, J. K. Fundamental Insights into the Reactivity and Utilization of Open Metal Sites in Cu(I)-MFU-4l. *Organometallics* **2019**, *38* (18), 3453−3459.
(34) Denysenko, D.; Volkmer, D. Cyclic Gas-Phase Heterogeneous Process in a Metal-Organic Framework Involving a Nickel Nitrosyl Complex. *Faraday Discuss.* **2017**, *201*, 101−112.
(35) Kitajima, N.; Fujisawa, K.; Morooka, Y. Tetrahedral Copper(II) Complexes Supported by a Hindered Pyrazolylborate. Formation of the Thiolato Complex, Which Closely Mimics the Spectroscopic Characteristics of Blue Copper Proteins. *J. Am. Chem. Soc.* **1990**, *112* (8), 3210−3212.
(36) Kitajima, N.; Fujisawa, K.; Tanaka, M.; Morooka, Y. X-Ray Structure of Thiolatocopper(II) Complexes Bearing Close Spectroscopic Similarities to Blue Copper Proteins. *J. Am. Chem. Soc.* **1992**, *114* (23), 9232−9233.
(37) Wright, A. M.; Wu, G.; Hayton, T. W. Structural Characterization of a Copper Nitrosyl Complex with a {CuNO} 10 Configuration. *J. Am. Chem. Soc.* **2010**, *132* (41), 14336−14337.
(38) Bower, J. K.; Sokolov, A. Y.; Zhang, S. Four-Coordinate Copper Halonitrosyl {CuNO}10 Complexes. *Angew. Chem., Int. Ed.* **2019**, *58* (30), 10225−10229.
(39) Xiao, B.; Wheatley, P. S.; Zhao, X.; Fletcher, A. J.; Fox, S.; Rossi, A. G.; Megson, I. L.; Bordiga, S.; Regli, L.; Thomas, K. M.; et al. High-Capacity Hydrogen and Nitric Oxide Adsorption and Storage in a Metal-Organic Framework. *J. Am. Chem. Soc.* **2007**, *129* (5), 1203−1209.
(40) Kalita, A.; Kumar, P.; Deka, R. C.; Mondal, B. First Example of a Cu(I)-(H2-O,O)Nitrite Complex Derived from Cu(II)-Nitrosyl. *Chem. Commun.* **2012**, *48* (9), 1251−1253.
(41) Mohamed, M. H.; Yang, Y.; Li, L.; Zhang, S.; Ruffley, J. P.; Jarvi, A. G.; Saxena, S.; Veser, G.; Johnson, J. K.; Rosi, N. L. Designing Open Metal Sites in Metal-Organic Frameworks for Paraffin/Olefin Separations. *J. Am. Chem. Soc.* **2019**, *141* (33), 13003−13007.
(42) Ruggiero, C. E.; Carrier, S. M.; Antholine, W. E.; Whittaker, J. W.; Cramer, C. J.; Tolman, W. B. Synthesis and Structural and Spectroscopic Characterization of Mononuclear Copper Nitrosyl Complexes: Models for Nitric Oxide Adducts of Copper Proteins and Copper-Exchanged Zeolites. *J. Am. Chem. Soc.* **1993**, *115* (24), 11285−11298.

https://dx.doi.org/10.1021/jacs.0c12134
J. Am. Chem. Soc. XXXX, XXX, XXX−XXX

(43) Woollard-Shore, J. G.; Holland, J. P.; Jones, M. W.; Dilworth, J. R. Nitrite Reduction by Copper Complexes. *Dalt. Trans.* **2010**, *39* (6), 1576−1585.
(44) Lionetti, D.; De Ruiter, G.; Agapie, T. A Trans-Hyponitrite Intermediate in the Reductive Coupling and Deoxygenation of Nitric Oxide by a Tricopper-Lewis Acid Complex. *J. Am. Chem. Soc.* **2016**, *138* (15), 5008−5011.

https://dx.doi.org/10.1021/jacs.0c12134
J. Am. Chem. Soc. XXXX, XXX, XXX−XXX